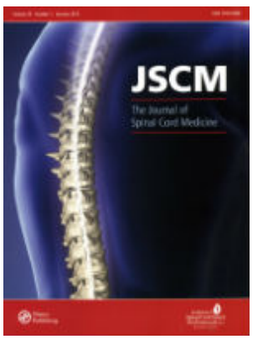

The Journal of Spinal Cord Medicine

ISSN: (Print) (Online) Journal homepage: https://www.tandfonline.com/loi/yscm20

Whole body measurements using near-infrared spectroscopy in a rat spinal cord contusion injury model

Brianna Kish, Seth Herr, Ho-Ching (Shawn) Yang, Siyuan Sun, Riyi Shi & Yunjie Tong

To cite this article: Brianna Kish, Seth Herr, Ho-Ching (Shawn) Yang, Siyuan Sun, Riyi Shi & Yunjie Tong (2021): Whole body measurements using near-infrared spectroscopy in a rat spinal cord contusion injury model, The Journal of Spinal Cord Medicine, DOI: 10.1080/10790268.2021.1911504

To link to this article: https://doi.org/10.1080/10790268.2021.1911504

Published online: 23 Apr 2021.

Research Article

Whole body measurements using near-infrared spectroscopy in a rat spinal cord contusion injury model

Brianna Kish [1], Seth Herr[2], Ho-Ching (Shawn) Yang [1], Siyuan Sun[2], Riyi Shi [1,2], Yunjie Tong [1]

[1]Weldon School of Biomedical Engineering, Purdue University, West Lafayette, Indiana, USA, [2]Center for Paralysis Research and Department of Basic Medical Sciences, College of Veterinary Medicine, Purdue University, West Lafayette, Indiana, USA

Background: Spinal cord injuries cause great damage to the central nervous system as well as the peripheral vasculature. While treatments for spinal cord injury typically focus on the spine itself, improvements in the function of the peripheral vasculature after spinal cord injury have shown to improve overall neurological recovery.
Objective: This study focused on the use of near-infrared spectroscopy (NIRS) as a mode to monitor cerebral and peripheral vascular condition non-invasively during the recovery process.
Design: Animal research study.
Methods: Rats underwent spinal contusion or sham injury and relative concentrations of de-/oxyhemoglobin (Δ[HbO]/Δ[Hb]) over time were measured over the cerebral, spinal, and pedal regions via NIRS. Correlational relationships across the body were determined. Rats received 1 NIRS measurement before injury and 3 after injury: 4, 7, and 14 days post.
Results: Correlational relationships between signals across the body, between animals with and without spinal cord injury, indicate that NIRS was able to detect patterns of vascular change in the spine and the periphery occurring secondary to spinal cord injury and evolving during subsequent recovery. Additionally, NIRS determined an overall correlational decrease within the central nervous system, between spinal and cerebral measurements.
Conclusion: NIRS was able to closely reflect physiologic changes in the rat during recovery, demonstrating a promising method to monitor whole body hemodynamics after spinal cord injury.

Keywords: Near infrared spectroscopy, spinal cord injury, blood flow, peripheral

Introduction

Spinal cord injuries (SCI) can cause lifelong debilitation and loss of nerve function.[1,2] Paralysis and other complications stem from the initial impact to the cord (primary injury), but persistent complications also arise from secondary injury, where chemical and cellular cascades lead to neuronal cell dysfunction and death long after injury. Specifically, inflammation, excitotoxicity, ischemia, hypoxia, and reactive aldehydes are all known to contribute to this cell death and continuous clinical complications.[1–10] Apart from paralysis, patients often suffer from neuropathic pain, bowl and bladder disfunction, obesity (lack of movement), and are at significantly higher risk for developing a neurodegenerative disease.[2,11] Furthermore, damage to the spinal sympathetic nervous system disrupts its control over caudal peripheral vasculature as well, causing a variety of vascular irregularities such as chronic hypotension, decreased vessel diameter and blood flow, increased vascular resistance and shear stress, and hypersensitivity to vasoconstrictive agents.[12–17] Together these changes can cause endothelial damage and acute bouts of blood pressure dysregulation and hypotension,

Correspondence to: Yunjie Tong, Weldon School of Biomedical Engineering, Purdue University, 206 S. Martin Jischke Drive, West Lafayette, IN 47907-2032, USA. E-mail: tong61@purdue.edu

Color versions of one or more of the figures in the article can be found online at www.tandfonline.com/yscm.

DOI 10.1080/10790268.2021.1911504

increasing the risk for cardiovascular disease and impairing recovery.[18]

The key to providing treatment able to influence secondary injury is consistent, reliable monitoring during the secondary phase to assess patient condition. Specifically, monitoring of a patient's vascular health and function has allowed for the intervention of targeted treatments that have shown to reduce the risk of permanent damage. Following initial surgical interventions such as spinal cord decompression to reduce pressure generated by hemorrhage in the spinal cord, restoration and strict maintenance of the patient's hemodynamics, i.e. blood flow and mean arterial pressure, especially to the site of injury and below, have been shown to significantly improve the outcome of a patient's neurological recovery.[19–21] Therefore, a reliable, noninvasive monitoring system will allow physicians to continuously assess vascular condition and determine if further surgical intervention or treatment is warranted for ensuring cord pressure relief and adequate blood flow.[22]

Near infrared spectroscopy (NIRS) is a diffuse optical imaging tool used for measuring the relative concentrations of oxyhemoglobin (Δ[HbO]) and deoxyhemoglobin (Δ[Hb]). Though blood flow is believed to be the predominant contributing factor in the NIRS signal, with increases of flow corresponding to an increase in Δ[HbO] and decrease in Δ[Hb], changes in blood volume and metabolic rate impact the signal as well, altogether reflecting complex hemodynamic changes. NIRS is a low cost, portable optical technology easily adaptable to record real-time physiologic changes from many locations over the body at once with high temporal resolution. While the system can act invasively, it also works noninvasively, allowing for examinations over long periods of time. Additionally, the system is easily set up and operated, making it ideal for quick and accurate measurements. Together, NIRS is a promising technique for assessing hemodynamic changes in SCI models.

NIRS was first used by Macnab *et al.* to monitor spinal cord hemodynamics in an animal model.[23] Subsequently, NIRS has been used in both animals and humans, primarily as a real-time indicator of ischemia and hypoxia.[24–28] Blood flow changes, i.e. ischemia/hypoxia, precede neurological damage, therefore NIRS can act as a warning to determine when or if counter actions are needed before permanent damage sets in. Similarly, some clinical trials have used NIRS measurements on the spinal cord and surrounding musculature to notify of possible ischemia during major surgeries requiring artery ligation.[29–34] Recently, using spinal contusion models, NIRS was successfully used as a monitoring system both invasively and noninvasively to detect induced acute alterations of mean arterial pressure post-SCI.[35,36] While research to date is limited, NIRS has shown great promise as a method for hemodynamic assessment, and hence, potentially offers a means for reducing or even preventing paralysis due to 'secondary injury' following SCI. However, these studies limit NIRS to the period of treatment application and focus solely on the spinal cord or directly affected tissues.

For the best use of noninvasive NIRS as a diagnostic/preventative tool, signals in the whole body should be considered. For this reason, we focused on spontaneous low frequency oscillations (sLFOs, $0.01 \sim 0.1$ Hz) found in the NIRS signal. These sLFOs represent systemic hemodynamic fluctuations in the body, which are related to vasomotion that helps move the blood in the arteries. It is known that in the resting state, sFLOs in NIRS signals are widely observed throughout the body, including the brain and periphery. They are highly correlated, especially between symmetric sites of the body, i.e. left and right brain, peripheries.[37] Therefore, we hypothesize that damage to the spinal vasculature and nervous system from SCI and the subsequent decrease of vascular control will disrupt these sLFOs, decreasing signal correlation.

The purpose of this study was to understand the hemodynamic changes and their correlations from multiple locations, including the spine, the brain, and periphery before and after SCI. Focus was placed on whole body signals to determine how hemodynamics are affected by SCI (1) at the central (i.e. brain, spine) and the peripheral sites, and (2) from above and below the injury. Because NIRS is a non-invasive technology, we can examine the long-term effects on hemodynamics during the recovery process though the secondary phase of SCI and their relationship to vascular health.

Materials and methods

Protocol

Approval for Animal Study (Protocol# 1111000095)

The study was conducted with 8 male Sprague Dawley rats: 4 rats in the SCI group and 4 rats in the sham group. One sham rat was excluded as it did not survive anesthesia. Spinal cord injury was achieved through a moderate contusion model using a NYU weight drop impactor, set at 25 mm drop height. Anesthesia was first administered intraperitoneally (IP) with a dosage of 80 mg/kg of ketamine and

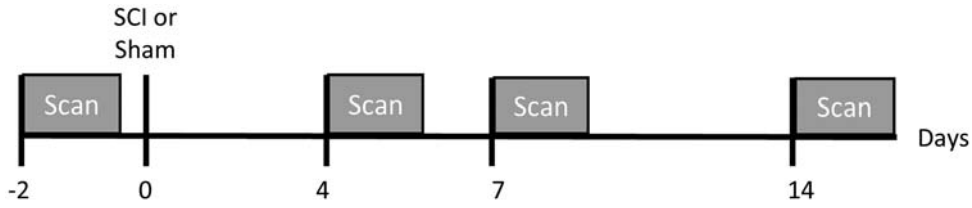

Figure 1 Experimental Protocol. Scans 2 days prior to SCI and 4, 7, and 14 days post SCI. Scan length: ~5 min.

10 mg/kg of xylazine. Sham rats received the laminectomy, but the cord was left uninjured. After injury, rats were sutured and carefully monitored for weight, bladder control, pain, and typical recovery.

NIRS data collection occurred 2 days prior to surgery and 4, 7, and 14, days post-operation (Fig. 1). The same anesthesia protocol was used during scans. Prior to scanning, hair on the head and back was removed to improve signal quality. Each scan lasted about 5 min. All animals were euthanized by CO2 gas after study completion.

NIRS data acquisition

The CW NIRS system (NIRScoutXP NIRx Medizintechnik GmbH; Berlin, Germany) was used to measure relative Δ[HbO] and Δ[Hb]. This system uses laser sources, each combining two wavelengths (785 and 830 nm). A series of probe holders were built for NIRS measurement (Fig. 2a). Rats were first secured in a stereotaxic device to keep the head level. An accompanying attachment was created to fit into the device and affix NIRS probes on the rat's head (Fig. 2b), including three NIRS channels (one source and three detectors), left and right hemisphere probe source-detector distance 1.3 cm and median probe source-detector distance 2 cm.

Additionally, a stiff cloth vest with an adjustable Velcro strap was sewn with holes cut out to hold NIRS probes with a set inter-probe distance, allowing for consistent probe placement over the spinal region

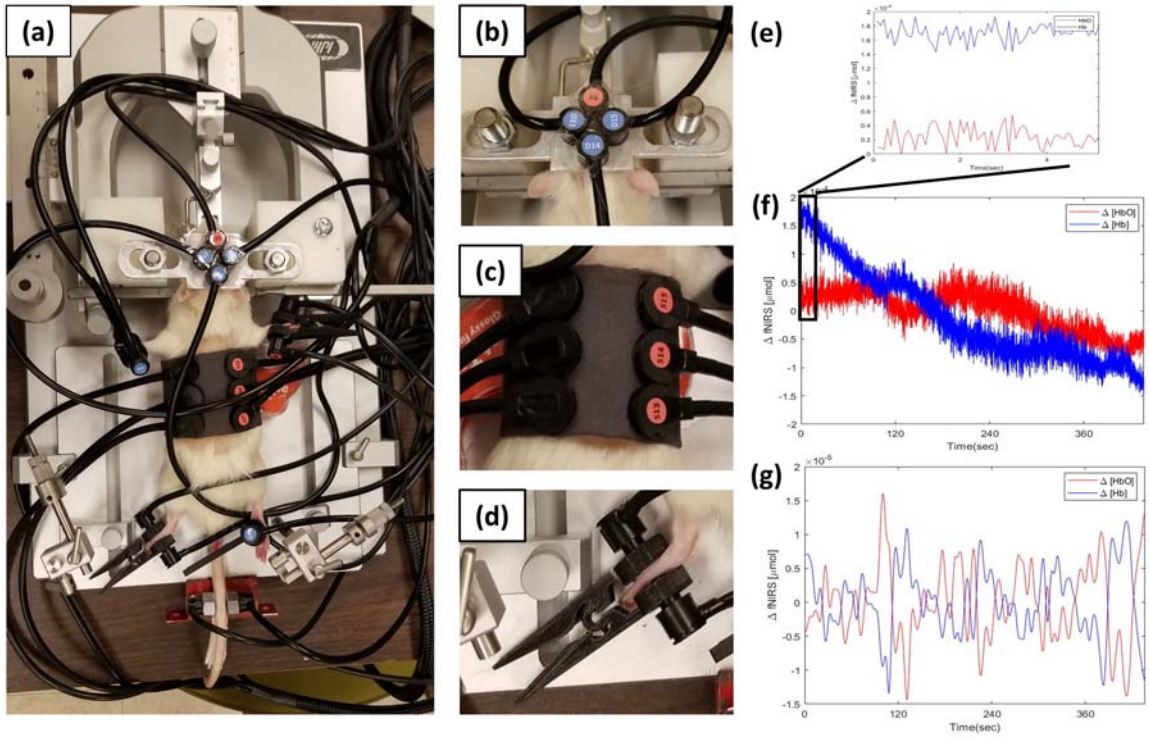

Figure 2 Experimental Configuration and Data Processing. (a) Anesthetized rat in NIRS setup, with head secured by a stereotaxic device (b) Head Device: 1 source, 3 detectors (c) Spinal Vest: 3 sources (red dots), 3 detectors (d) 3D Printed Foot Clamp: 1 source, 1 detector (e) 5 s interval of raw data in (f), heartbeat seen at ~3.5 Hz (f) Full ~7 min raw, unfiltered data (1 channel) (g) Data from (f) filtered to 0.01–0.1 Hz (1 channel).

across scans (Fig. 2c). The vest holds 1 column of three sources and 1 column of three detectors, each paired horizontally, creating 3 channels with a source-detector distance of 3 cm. The vest was wrapped around the rat's mid-section and affixed so that the center channel rested above the affected vertebrae. Peripheral data (hindlimb and forelimb paws, and tail) were collected from each foot using 3D printed clasps (one channel each), holding 1 source and detector each (Fig. 2d). An additional channel was placed on the tail using a metal ring around each probe and a strong magnet underneath the tail. Probes were readjusted until a good signal quality, i.e. a visible heartbeat could be seen (Fig. 2 e-g), was reached before scanning.

Data analysis

All NIRS data were processed using the nirsLAB analysis package (v2016.05, NIRx Medical Technologies, LLC.; Los Angeles, USA) and MATLAB (MATLAB 2018b, The MathWorks Inc., Natick, MA, 2000).[38] A zero-delay band-pass filter (0.01–0.1 Hz, 3rd order) was applied to examine the low frequency component of each signal.

Correlation values were determined between each channel for both Δ[HbO] and Δ[Hb]. Tail signals were universally excluded as the signal quality was consistently poor. Correlation values were grouped into different categories: spinal-spinal, cerebral-spinal, feet-feet, cerebral-feet, spinal-feet, and analyzed over the four scans with a one-way ANOVA test ($P < 0.05$) for statistical significance.

Results

Full body signal

Figure 3 shows an example of the whole body NIRS measurement (filtered) for a single rat pre-surgery (healthy). As shown in Fig. 3d-f, the center back channel (red square) is placed above the injury location so that there are spinal recordings from above and below the injury as well. Hindlimb and forelimb paws and tail signals, defined here as "peripheral signals," follow the divide of the spinal channels to have recording from above and below the injury. Prior to injury, high correlations were found between the three head channels ($r_{avg} = 0.8514$, $P < 0.05$) as well as among the three back channels ($r_{avg} = 0.8599$, $P < 0.05$). Peripheral channels, while similar, are not as highly correlated ($r_{avg\_feet} = 0.2374$, $P < 0.05$, $r_{avg\_feet\text{-}tail} = 0.1314$, $P < 0.05$). Consistent high correlation values among head channels were seen across the entire 2-week scanning period for both SCI and sham rats (See Appendix Fig. A1).

Spinal correlation

In correlation values between the three spinal channels, a significant drop ($P < 0.05$) in Δ[HbO] correlation values occurs from pre-surgery values to 4- and 7-days post operation in SCI rats (Table 1), followed by a rise at 14 days (Fig. 4a). Δ[Hb] values exhibit a similar pattern, but there are no significant changes. Sham rats showed no significant changes overall.

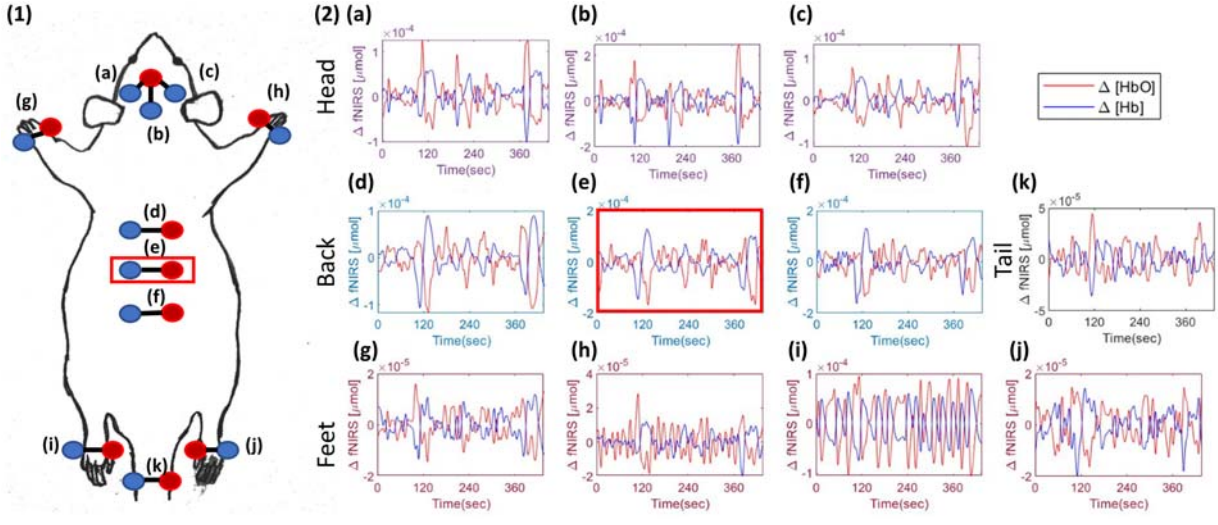

Figure 3 Example filtered NIRS data (1 rat) from before injury. Relative location of injury highlighted with red box in (1) and (2). (1) NIRS probe design: 9 sources (red circles) and 11 detectors (blue circles), 11 channels corresponding to plotted graphs in 2 (black lines). (a-c) Three head channels: left, middle, right (d-f) Three back channels: lower, middle, upper. (g-j) Four feet channels: front left, front right, back left, back right (k) Tail channel.

Table 1 Correlational values for signal groupings and paired statistical values for SCI/Sham Δ [HbO].

Δ [HbO]		Average R				s	F	*P*
		Before	4 Days	7 Days	14 Days			
SCI	Spinal	0.8004	0.3063	0.4211	0.5331	0.3060	5.73	0.005
	Cerebro-spinal	0.5382	0.4419	0.2942	0.2459	0.2367	11.62	0.001
	Feet-feet	0.2483	0.1615	0.1528	0.3761	0.2653	3.66	0.05
	Spinal-feet	0.3498	0.1777	0.2580	0.3037	0.2531	4.03	0.01
Sham	Spinal	0.7442	0.5792	0.6607	0.5952	0.2339	0.93	0.5
	Cerebro-spinal	0.4914	0.5339	0.4672	0.3577	0.2105	3.45	0.05
	Feet-feet	0.3211	0.1223	0.4053	0.2055	0.3043	3.03	0.05
	Spinal-feet	0.3986	0.1913	0.3899	0.1873	0.2096	11.49	0.001

Cerebral spinal correlation

Correlation values between the three head channels and 3 back channels showed a significant drop ($P < 0.05$) in both Δ[HbO] and Δ[Hb] correlation values from the before and 4 days post-op to the 7- and 14-days post-op in SCI rats (Table 1, Table 2) (Fig. 5a, b). Sham rats showed a reversed pattern to the back-back SCI correlation, with an increase in correlation at 4 days, followed by a decrease with a significant drop in correlation values at 14 days (Fig. 5c, d).

Peripheral correlation

From the peripheral channels, a significant rise is seen in the Δ[HbO] correlation values between the four feet channels at 14 days post-op in SCI rats (Table 1) (Fig. 6a), ($r_{SCI\_avg[HbO]} = 0.2347$, $r_{SCI\_avg[Hb]} = 0.2692$, $r_{Sham\_avg[HbO]} = 0.2636$, $r_{Sham\_avg[Hb]} =$

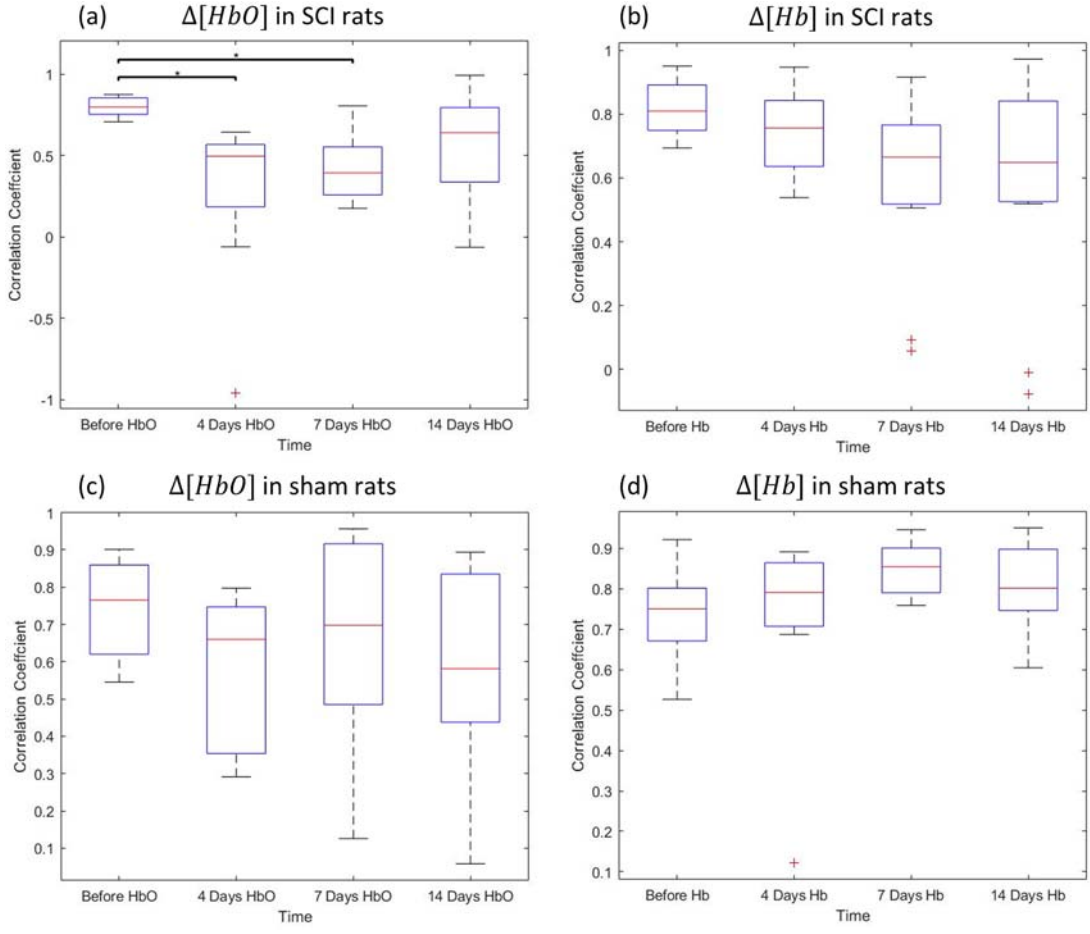

Figure 4 Correlation between three back channels over time. (a) Δ[HbO] in SCI rats (b) Δ[Hb] in SCI rats (c) Δ[HbO] in sham rats (d) Δ[Hb] in sham rats.

Table 2 Correlational values for signal groupings and paired statistical values for SCI/Sham Δ [Hb].

Δ [Hb]		Average R				s	F	*P*
		Before	4 Days	7 Days	14 Days			
SCI	Spinal	0.8188	0.7484	0.5889	0.5919	0.2266	3.10	0.05
	Cerebro-spinal	0.6069	0.6787	0.4373	0.3639	0.1995	19.28	0.001
	Feet-feet	0.3020	0.1082	0.1494	0.2731	0.2848	2.61	0.1
	Spinal-feet	0.4365	0.2461	0.2874	0.3241	0.3053	3.44	0.05
Sham	Spinal	0.7320	0.7179	0.8474	0.8016	0.1495	1.48	0.001
	Cerebro-spinal	0.5818	0.6433	0.5966	0.4231	0.1929	6.65	0.001
	Feet-feet	0.3221	0.1492	0.4258	0.1818	0.3007	3.28	0.05
	Spinal-feet	0.3236	0.2620	0.4360	0.1863	0.2457	6.64	0.001

0.2855). Correlation values between the four feet channels and the three back channels showed a drop in values from before SCI to 4 days post-op in both Δ [HbO] and Δ[Hb] (Table 1, Table 2) (Fig. 7a,b). Both groups depict a similar pattern to spinal-spinal correlation values of a correlation drop 4 days after surgery and SCI followed by a slow recovery. Sham rats generally saw a decrease in correlation at 4 days, followed by an increase at 7 days, and eventual decrease at 14 days. Correlation values between feet and head channels showed little change over time (Appendix Fig. A2).

Discussion

This study characterized NIRS signals obtained non-invasively in a rat spinal cord injury model and sham control animals and examined whole body hemodynamic correlations over an extended period post-injury. Clear patterns of correlational decreases in Δ [HbO] and Δ[Hb] signals after injury followed by a

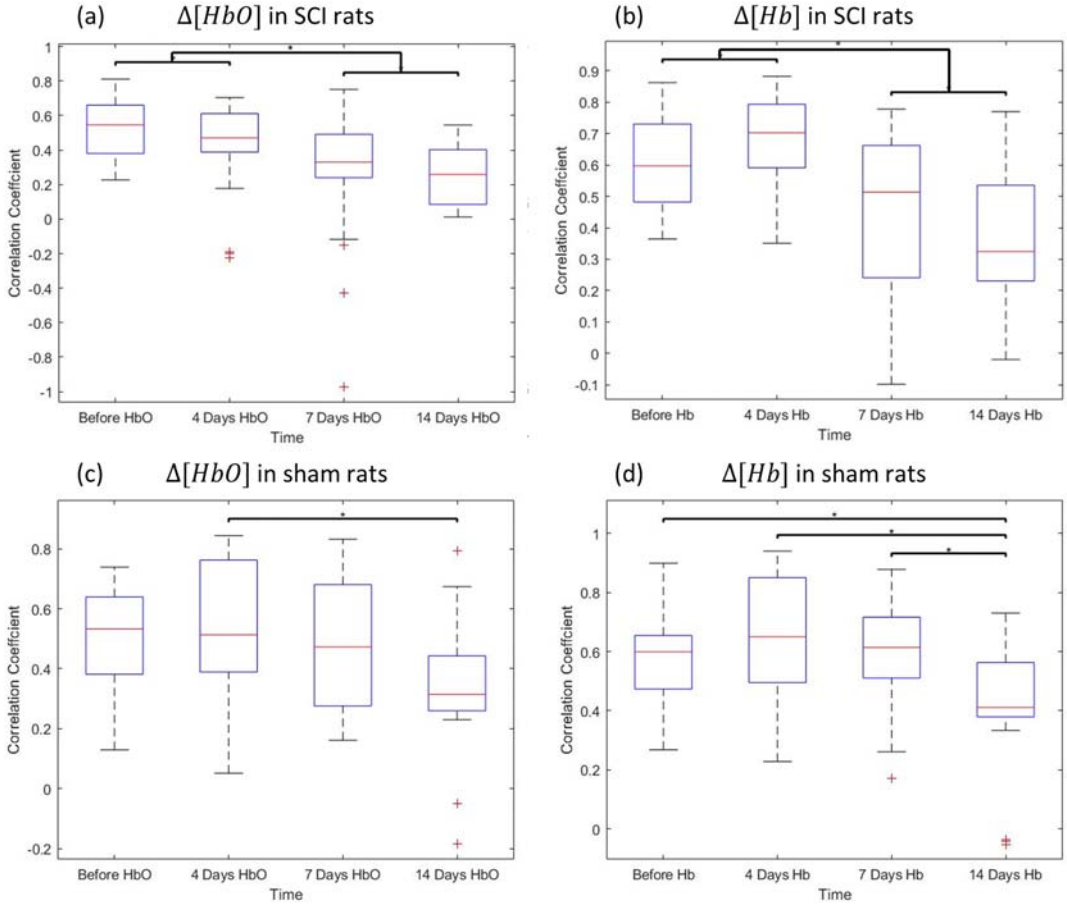

Figure 5 Correlation between three back channels and three head channels over time. (a) Δ[HbO] in SCI rats (b) Δ[Hb] in SCI rats (c) Δ[HbO] in sham rats (d) Δ[Hb] in sham rats.

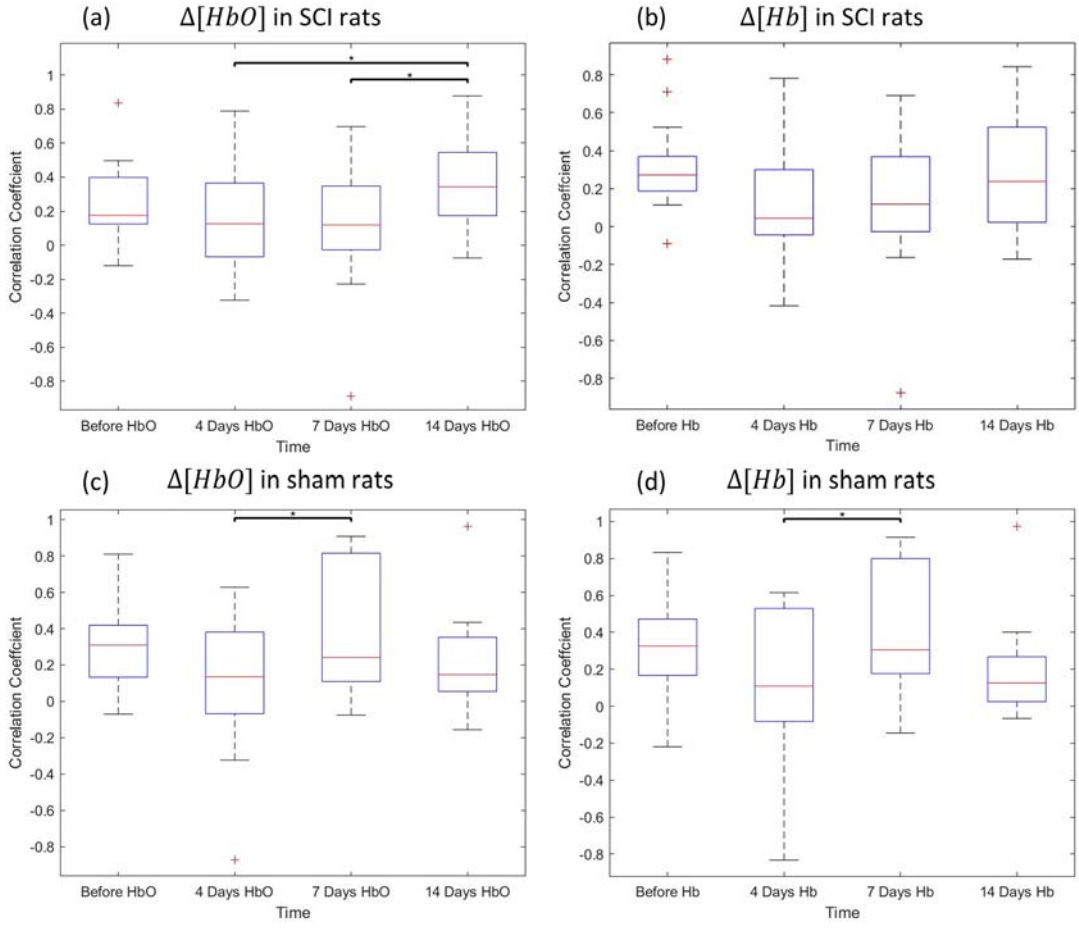

Figure 6 Correlation between four feet channels over time. (a) Δ[HbO] in SCI rats (b) Δ[Hb] in SCI rats (c) Δ[HbO] in sham rats (d) Δ[Hb] in sham rats.

slow recovery to pre-injury values could be seen when examining the spinal cord and periphery in SCI rats. Continued decreases could be seen in cerebral-spinal/cerebral-feet signals as well. These patterns of change reflected physiologic changes known to occur in the vasculature due to SCI, thus supporting the use of NIRS as a metric for monitoring following SCI, to guide treatment to minimize 'secondary injury' and potentially optimize recovery.[15,39,40]

Spinal cord recovery

Correlation coefficients from the spinal signals above, over, and below the injury were calculated to observe consistency of spinal hemodynamics. From the uninjured spinal cords to 4 days post injury, a significant decrease can be seen in Δ[HbO] (Fig. 4a). From 4 to 7 days post the correlation coefficients rise, though remaining significantly lower than uninjured. At 14 days post SCI, correlation values were non-significantly different from uninjured values, which may represent hemodynamic recovery in those rats. Previous studies showed that SCI causes the destruction of blood vessels at the injury epicenter, followed by a period of rapid angiogenesis, with vasculature reaching reformation through the epicenter after 7 days and reorganization and pruning evident at 14 days post SCI, closely mirroring our results.[39,40] It is worth noting that in the sham rats, a laminectomy was still performed, which certainly would cause vascular trauma. This could explain the decrease in Δ[HbO] in both sham and SCI rats. However, the trend of recovery was much more obvious in the case of SCI in both Δ[HbO] and Δ[Hb], indicating the reliability of NIRS signals in reflecting the SCI time course.

Impact on cerebral and peripheral signals

Throughout the testing period, cerebral channels retained high correlation values to one another, but gradually decreased in correlation to spinal channels. Consistent high correlation values among the cerebral channels indicated that the SCI did not have significant impact on the cerebrovasculature. From a practical

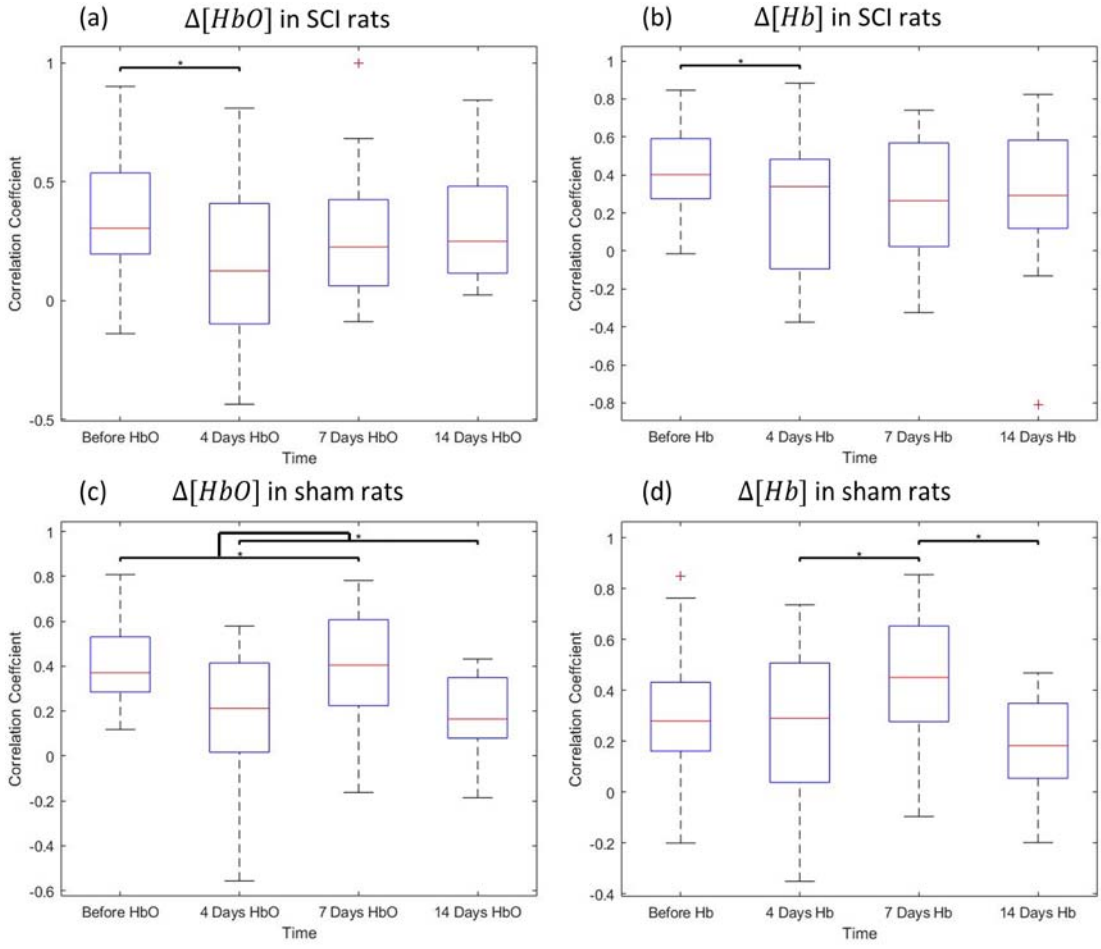

Figure 7 Correlation between four feet channels and 3 back channels over time. (a) Δ[HbO] in SCI rats (b) Δ[Hb] in SCI rats (c) Δ[HbO] in sham rats (d) Δ[Hb] in sham rats.

point of view, the un-altered cerebral signal can serve as a reference to evaluate the changes in the spinal cord and peripheries before and after the SCI. A significant correlation decrease (cerebral-spinal) was found in both Δ[HbO] and Δ[Hb] from pre and 4-days post injury to 7- and 14-days post injury (Fig. 5a, b). A similar pattern can be seen in cerebral-feet correlation values, though significant differences were only found in Δ[Hb] (See Appendix Fig. A2). Together, these two results might suggest that even after vasculature regenerates in the spine and regional hemodynamic recovery is evident, whole body (long-distance) hemodynamic homeostasis might take much longer to occur.

Further examination of the peripheral signals showed that both feet-feet correlation values and feet-spinal correlation values displayed similar patterns to spinal correlations; a drop at 4-days post followed by a slow rise. It is worth noting that peripheral vascular health has been proven to decrease in SCI patients in the upper and lower limbs, with stronger changes dependent on the injury location.[15,41,42] Acute damage to the nervous system deregulates muscle control, resulting in persistent hypotension, while chronic damage due to inactivity and reduced metabolic demand are known to decrease arterial diameter and blood flow and increase blood velocity, vascular resistance, and sensitivity to hypertensive agents.[12–16] These changes can induce periods of unstable blood pressure and increase shear stress, which can cause endothelial damage in the affected limbs, which in theory, should decrease peripheral correlation values. However, when comparing front paw to back paw signals, the same pattern can be seen as in total feet-feet and spinal correlations (See Appendix Fig. A3). Altogether, this could indicate that the primary factor in SCI recovery discernible by NIRS, when examining the spine and periphery alone, is the restoration of spinal function, however when compared to the cerebrovasculature, influence of permanent damage can be seen as correlation values failed to recover. However, average feet-feet correlation values were low

overall, both before and after SCI. This may be due to design of the probe holder that did not optimize the light coupling between probes and the tissues.

Advantage of longitudinal monitoring of SCI

The majority of current NIRS studies on the impact of SCI have limited themselves to monitoring for the onset of hypoxia and ischemia in order to administer treatment immediately to prevent neuronal deficits.[23–28] Capitalizing on the ability of NIRS to perform non-invasive measurements and record from the entire body simultaneously, it can be used as a long-term monitoring system for SCI and possibly a metric for vascular health. Arteries within the lower limbs have been shown to deteriorate in SCI patients over time.[15,41,42] Both CT and MRI have been used to image spinal health after injury, but these typically are not used to assess peripheral recovery.[43] As compared to these methods, NIRS is a low-cost procedure, easily adaptable to fit the patient condition, and has demonstrated promise of detecting injury induced hemodynamic changes. Few studies have determined NIRS' ability to detect acute bouts of fluctuating mean arterial pressure after SCI already.[35,36] Its use could provide real-time monitoring of artery regeneration in the spine and peripheral arterial condition to aide in the prevention vascular damage and hypoxia.

Limitations and future studies

Though the non-invasive nature of NIRS allows us to monitor animals for prolonged periods, NIRS is prone to physiological noise from superficial layers (e.g. skin, skull). For example, 1 SCI rat experienced some fluid swelling above the injury epicenter (evident at 4 days, but decreased at 7 days), which can decrease the signal quality. Additionally, this study had a small sample size. However, clear correlational patterns were still observed in SCI rats and differed from sham rats. These patterns were seen both centrally and in the periphery, however future experiments will improve upon the peripheral probe holder design to reduce signal noise, increase the average correlation values overall, increase sample size, and include the tail channel.

NIRS provides an overall measurement of an individual's hemodynamics through the relative concentrations of de/oxyhemoglobin and oxygen saturation. Clear patterns were seen in the results, however the combination of diffuse correlation spectroscopy (DCS) with NIRS is worth investigating as validation of our results due to its ability to monitor microvascular cerebral and muscular blood flow precisely and oxygen consumption.[44,45]

Conclusion

This study demonstrated the use of NIRS to monitor cerebral, spinal, and peripheral hemodynamics and their correlation in rats before and after SCI as a method to assess vascular health. With its noninvasive nature and adaptability, NIRS is an ideal monitoring system for SCI and has shown to offer valuable hemodynamic information on vascular recovery in localized regions and the body as a whole. Future studies can combine NIRS with DCS to investigate microvascular blood flow and oxygen consumption of rats under SCI.

Disclaimer statements

Contributors None.

Funding Funding Research reported in this publication was supported with funds from the Purdue Institute for Integrative Neuroscience and NIH [1R21NS115094-01].

Conflicts of interest Authors have no conflict of interests to declare.

ORCID

Brianna Kish http://orcid.org/0000-0001-5906-1295
Ho-Ching (Shawn) Yang http://orcid.org/0000-0003-2670-1772
Riyi Shi http://orcid.org/0000-0002-7297-9428
Yunjie Tong http://orcid.org/0000-0001-6052-8913

References

1 Kwon BK, Tetzlaff W, Grauer JN, Beiner J, Vaccaro AR. Pathophysiology and pharmacologic treatment of acute spinal cord injury. Spine J 2004;4(4):451–64. doi:10.1016/j.spinee.2003.07.007.
2 Alizadeh A, Dyck SM, Karimi-Abdolrezaee S. Traumatic spinal cord injury: An overview of pathophysiology, models and acute injury mechanisms. Front Neurol 2019;10:282. doi:10.3389/fneur.2019.00282.
3 Agrawal SK, Fehlings MG. Mechanisms of secondary injury to spinal cord axons *in vitro*: role of Na+, Na+-K+-ATPase, the Na+-H+ exchanger, and the Na+-Ca2+ exchanger. J Neurosci 1996;16(2):545–52. doi:10.1523/jneurosci.16-02-00545.1996.
4 Li Y, *et al*. Pericytes impair capillary blood flow and motor function after chronic spinal cord injury. Nat Med 2017;23(6):733–41. doi:10.1038/nm.4331.
5 Hernandez-Gerez E, Fleming IN, Parson SH. A role for spinal cord hypoxia in neurodegeneration. Cell Death Dis 2019;10(11):1–8. doi:10.1038/s41419-019-2104-1.
6 Hamann K, Durkes A, Ouyang H, Uchida K, Pond A, Shi R. Critical role of acrolein in secondary injury following *ex vivo* spinal cord trauma. J Neurochem 2008;107(3):712–21. doi:10.1111/j.1471-4159.2008.05622.x.
7 Hamann K, Shi R. Acrolein scavenging: a potential novel mechanism of attenuating oxidative stress following spinal cord injury. J Neurochem 2009;111(6):1348–56. doi:10.1111/j.1471-4159.2009.06395.x.

8 Lin Y, Chen Z, Tang J, Cao P, Shi R. Acrolein contributes to the neuropathic pain and neuron damage after ischemic–reperfusion spinal cord injury. Neuroscience 2018;384:120–30. doi:10.1016/j.neuroscience.2018.05.029.

9 Shi R, Luo L. The role of acrolein in spinal cord injury. Appl Neurol 2006: 22–7. [cited 2020 August 29]. Available from https://www.psychiatrictimes.com/view/role-acrolein-spinal-cord-injury.

10 Shi R, Rickett T, Sun W. Acrolein-mediated injury in nervous system trauma and diseases. Mol Nutr Food Res 2011;55(9): 1320–31. doi:10.1002/mnfr.201100217.

11 Sezer N, Akkuş S, Uğurlu FG. Chronic complications of spinal cord injury. World J Orthop 2015;6(1):24–33. doi:10.5312/wjo.v6.i1.24.

12 Piepmeier JM, Lehmann KB, Lane JG. Cardiovascular instability following acute cervical spinal cord trauma. Cent Nerv Syst Trauma 1985;2(3):153–60. doi:10.1089/cns.1985.2.153.

13 Houtman S, Oeseburg B, Hopman MTE. Blood volume and hemoglobin after spinal cord injury. Am J Phys Med Rehabil 2000;79(3):260–5. doi:10.1097/00002060-200005000-00008.

14 Boot CRL, Groothuis JT, Van Langen H, Hopman MTE. Shear stress levels in paralyzed legs of spinal cord-injured individuals with and without nerve degeneration. J Appl Physiol 2002;92(6): 2335–40. doi:10.1152/japplphysiol.00340.2001.

15 De Groot PCE, Van Kuppevelt DHJM, Pons C, Snoek G, Van Der Woude LHV, Hopman MTE. Time course of arterial vascular adaptations to inactivity and paralyses in humans. Med Sci Sports Exerc 2003;35(12):1977–85. doi:10.1249/01.MSS.0000099088.21547.67.

16 Groothuis JT, Boot CR, Houtman S, van Langen H, Hopman MTE. Leg vascular resistance increases during head-up tilt in paraplegics. Eur J Appl Physiol 2005;94(4):408–14. doi:10.1007/s00421-005-1340-5.

17 West CR, Alyahya A, Laher I, Krassioukov A. Peripheral vascular function in spinal cord injury: A systematic review. Spinal Cord 2013;51(1):10–19. doi:10.1038/sc.2012.136.

18 Philpott AC, Lonn E, Title LM, Verma S, Buithieu J, Charbonneau F, Anderson TJ. Comparison of new measures of vascular function to flow mediated dilatation as a measure of cardiovascular risk factors. Am J Cardiol 2009;103(11):1610–15. doi:10.1016/j.amjcard.2009.01.376.

19 Fehlings MG, *et al*. Early versus delayed decompression for traumatic cervical spinal cord injury: results of the surgical timing in acute spinal cord injury study (STASCIS). Di Giovanni S, ed. PLoS One 2012;7(2):e32037. doi:10.1371/journal.pone.0032037.

20 Hawryluk G, *et al*. Mean arterial blood pressure correlates with neurological recovery after human spinal cord injury: analysis of high frequency physiologic data. J Neurotrauma 2015;32(24): 1958–67. doi:10.1089/neu.2014.3778.

21 Casha S, Christie S. A systematic review of intensive cardiopulmonary management after spinal cord injury. J Neurotrauma 2011;28(8):1479–95. doi:10.1089/neu.2009.1156.

22 Kong CY, *et al*. A prospective evaluation of hemodynamic management in acute spinal cord injury patients. Spinal Cord 2013; 51(6):466–71. doi:10.1038/sc.2013.32.

23 Macnab AJ, Gagnon RE, Gagnon FA. Near infrared spectroscopy for intraoperative monitoring of the spinal cord. Spine (Phila Pa 1976) 2002;27(1):17–20. doi:10.1097/00007632-200201010-00007.

24 LeMaire SA, *et al*. Transcutaneous near-infrared spectroscopy for detection of regional spinal ischemia during intercostal artery ligation: preliminary experimental results. J Thorac Cardiovasc Surg 2006;132(5):1150–5. doi:10.1016/j.jtcvs.2006.05.047.

25 Shadgan B, *et al*. Optical monitoring of spinal cord subcellular damage after acute spinal cord injury. In: Coté GL, (ed.) *Optical diagnostics and sensing XVIII: Toward point-of-care diagnostics*; 10501. SPIE; 2018: 20. doi:10.1117/12.2286551.

26 Kogler AS, *et al*. Fiber-optic monitoring of spinal cord hemodynamics in experimental aortic occlusion. Anesthesiology 2015;123 (6):1362–73. doi:10.1097/ALN.0000000000000883.

27 Suehiro K, Funao T, Fujimoto Y, Mukai A, Nakamura M, Nishikawa K. Transcutaneous near-infrared spectroscopy for monitoring spinal cord ischemia: an experimental study in swine. J Clin Monit Comput 2017;31(5):975–9. doi:10.1007/s10877-016-9931-8.

28 Mesquita RC, *et al*. Optical monitoring and detection of spinal cord ischemia. Coles JA, ed. PLoS One 2013;8(12):e83370. doi:10.1371/journal.pone.0083370.

29 Badner NH, Nicolaou G, Clarke CFM, Forbes TL. Use of spinal near-infrared spectroscopy for monitoring spinal cord perfusion during endovascular thoracic aortic repairs. J Cardiothorac Vasc Anesth 2011;25(2):316–19. doi:10.1053/j.jvca.2010.01.011.

30 Moerman A, Van Herzeele I, Vanpeteghem C, Vermassen F, François K, Wouters P. Near-infrared spectroscopy for monitoring spinal cord ischemia during hybrid thoracoabdominal aortic aneurysm repair. J Endovasc Ther 2011;18(1):91–5. doi:10.1583/10-3224.1.

31 Berens RJ, *et al*. Near infrared spectroscopy monitoring during pediatric aortic coarctation repair. Paediatr Anaesth 2006;16(7): 777–81. doi:10.1111/j.1460-9592.2006.01956.x.

32 Demir A, Erdemli Ö, Ünal U, Taşoğlu İ. Near-infrared spectroscopy monitoring of the spinal cord during type B aortic dissection surgery. J Card Surg 2013;28(3):291–4. doi:10.1111/jocs.12082.

33 Etz CD, *et al*. Near-infrared spectroscopy monitoring of the collateral network prior to, during, and after thoracoabdominal aortic repair: A pilot study. Eur J Vasc Endovasc Surg 2013;46 (6):651–6. doi:10.1016/j.ejvs.2013.08.018.

34 Boezeman RPE, Van Dongen EP, Morshuis WJ, Sonker U, Boezeman EHJF, Waanders FGJ, de Vries J-PPM. Spinal near-infrared spectroscopy measurements during and after thoracoabdominal aortic aneurysm repair: a pilot study. Ann Thorac Surg 2015;99(4):1267–74. doi:10.1016/j.athoracsur.2014.10.032.

35 Shadgan B, *et al*. Optical assessment of spinal cord tissue oxygenation using a miniaturized near infrared spectroscopy sensor. J Neurotrauma 2019;36(21):3034–43. doi:10.1089/neu.2018.6208.

36 Cheung A, *et al*. Using near-infrared spectroscopy to monitor spinal cord oxygenation in the injured spinal cord. In: Coté GL, (ed.) Optical diagnostics and sensing XX: Toward point-of-care diagnostics. Vol 11247. SPIE; 2020:8. doi:10.1117/12.2546577.

37 Tong Y, Hocke LM, Licata SC, Frederick B. Low-frequency oscillations measured in the periphery with near-infrared spectroscopy are strongly correlated with blood oxygen level-dependent functional magnetic resonance imaging signals. J Biomed Opt 2012; 17(10):1. doi:10.1117/1.jbo.17.10.106004.

38 Xu Y, Graber HL, Barbour RL. nirsLAB: A Computing Environment for fNIRS Neuroimaging Data Analysis. In: The Optical Society; 2014:BM3A.1. doi:10.1364/biomed.2014.bm3a.1.

39 Loy DN, Crawford CH, Darnall JB, Burke DA, Onifer SM, Whittemore SR. Temporal progression of angiogenesis and basal lamina deposition after contusive spinal cord injury in the adult rat. J Comp Neurol 2002;445(4):308–24. doi:10.1002/cne.10168.

40 Casella GTB, Marcillo A, Bunge MB, Wood PM. New vascular tissue rapidly replaces neural parenchyma and vessels destroyed by a contusion injury to the rat spinal cord. Exp Neurol 2002; 173(1):63–76. doi:10.1006/exnr.2001.7827.

41 Stoner L, Sabatier M, VanhHiel L, Groves D, Ripley D, Palardy G, McCully K. Upper vs lower extremity arterial function after spinal cord injury. J Spinal Cord Med 2006;29(2):138–46. doi:10.1080/10790268.2006.11753867.

42 Schmidt-Trucksass A, Schmid A, Brunner C, Scherer N, Zäch G, Keul J, Huonker M. Arterial properties of the carotid and femoral artery in endurance-trained and paraplegic subjects. J Appl Physiol 2000;89(5):1956–63. doi:10.1152/jappl.2000.89.5.1956.

43 Goldberg AL, Kershah SM. Advances in imaging of vertebral and spinal cord injury. J Spinal Cord Med 2010;33(2):105–16. doi:10.1080/10790268.2010.11689685.

44 Durduran T, Yodh AG. Diffuse correlation spectroscopy for non-invasive, micro-vascular cerebral blood flow measurement. Neuroimage 2014;85:51. doi:10.1016/j.neuroimage.2013.06.017.

45 Yu KG G. Diffuse correlation spectroscopy (DCS) for assessment of tissue blood flow in skeletal muscle: recent progress. Anat Physiol 2013;03(02):128. doi:10.4172/2161-0940.1000128.

Appendix

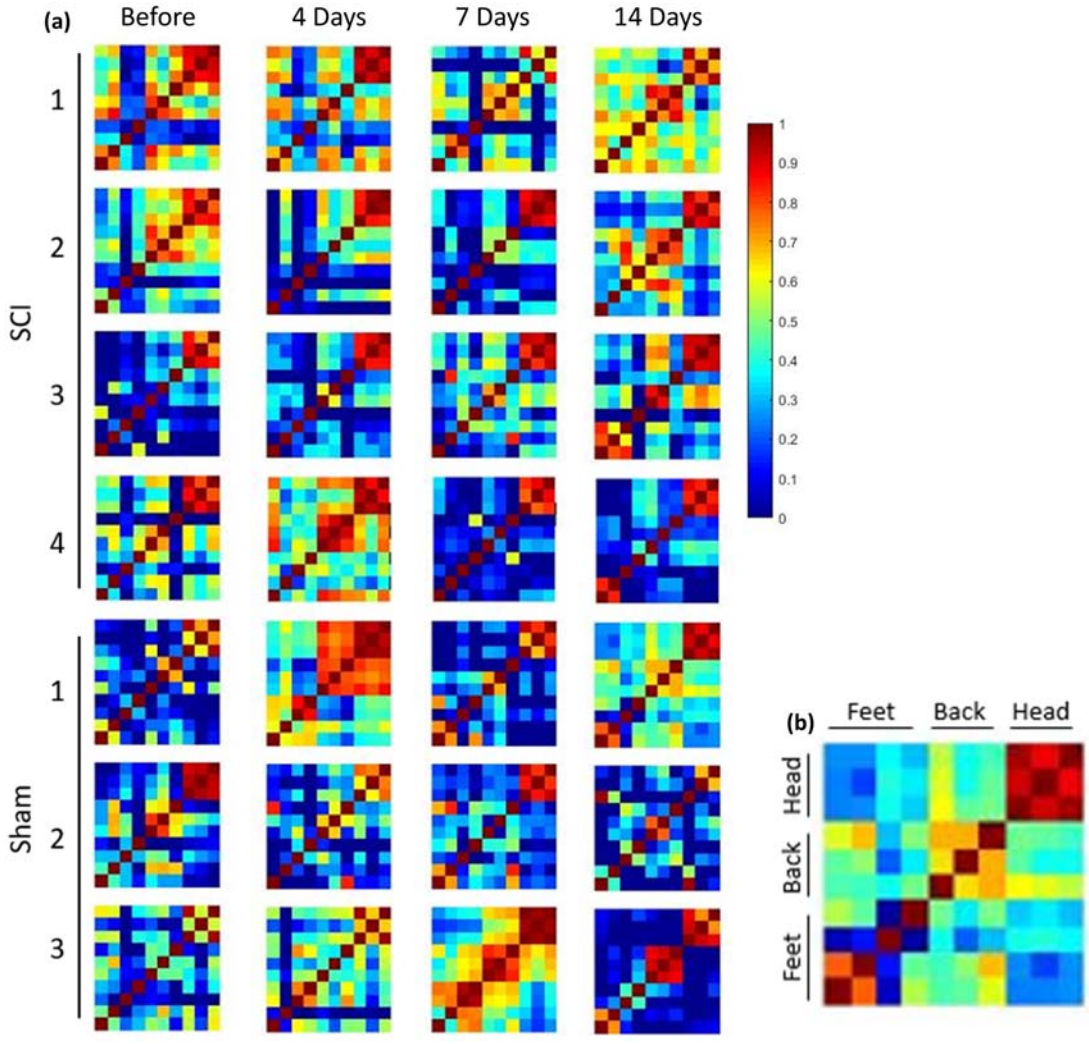

Figure A1 Correlation Maps of Δ[HbO] Over Time. (a) Each map shows the correlation values for each channel combination. The top 4 rows show SCI rats, and the bottom three rows show sham rats. Each column corresponds to data collected before SCI, 4 days post, 7 days post, and 14 days post SCI respectively. (b) Enlarged correlation map of Sham rat 1, 14 Days with channel location labeled.

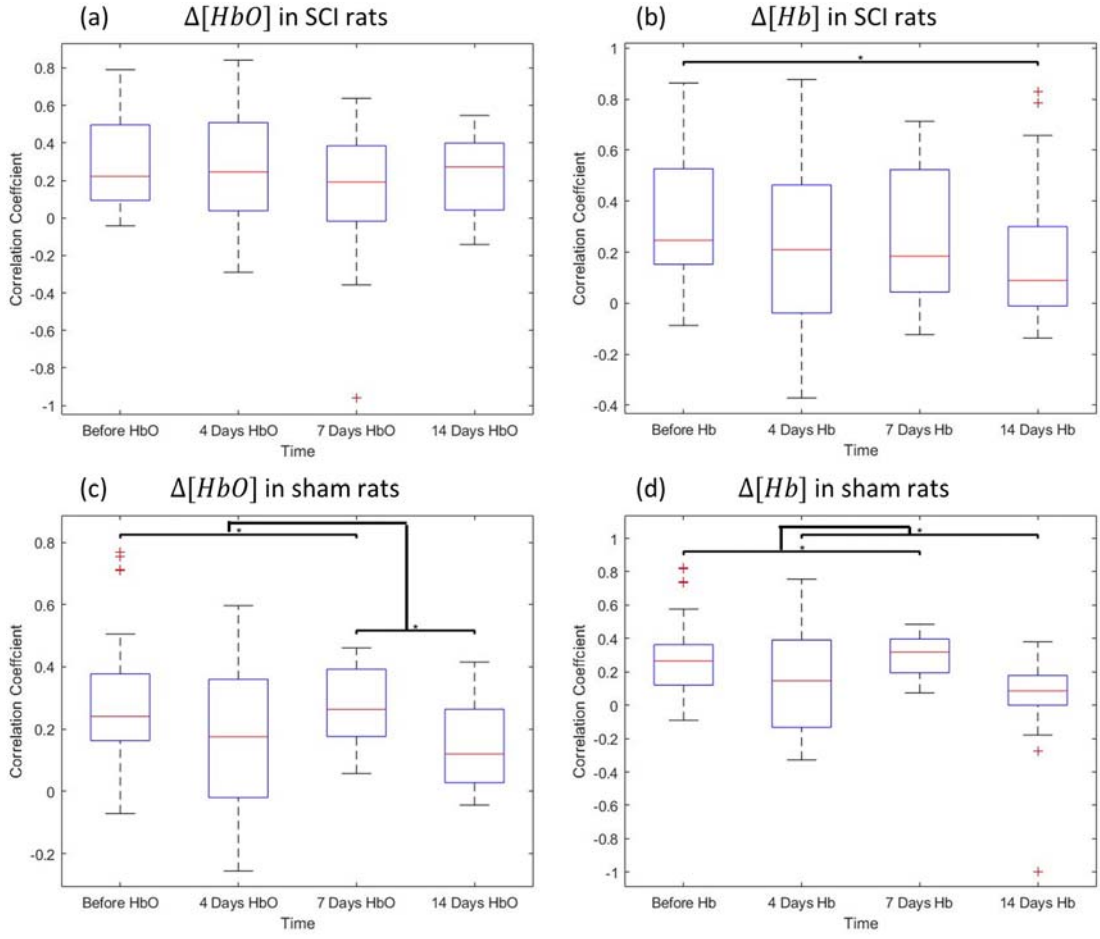

Figure A2 Correlation between four feet channels and 3 head channels over time. (a) Δ[HbO] in SCI rats (b) Δ[Hb] in SCI rats (c) Δ[HbO] in sham rats (d) Δ[Hb] in sham rats.

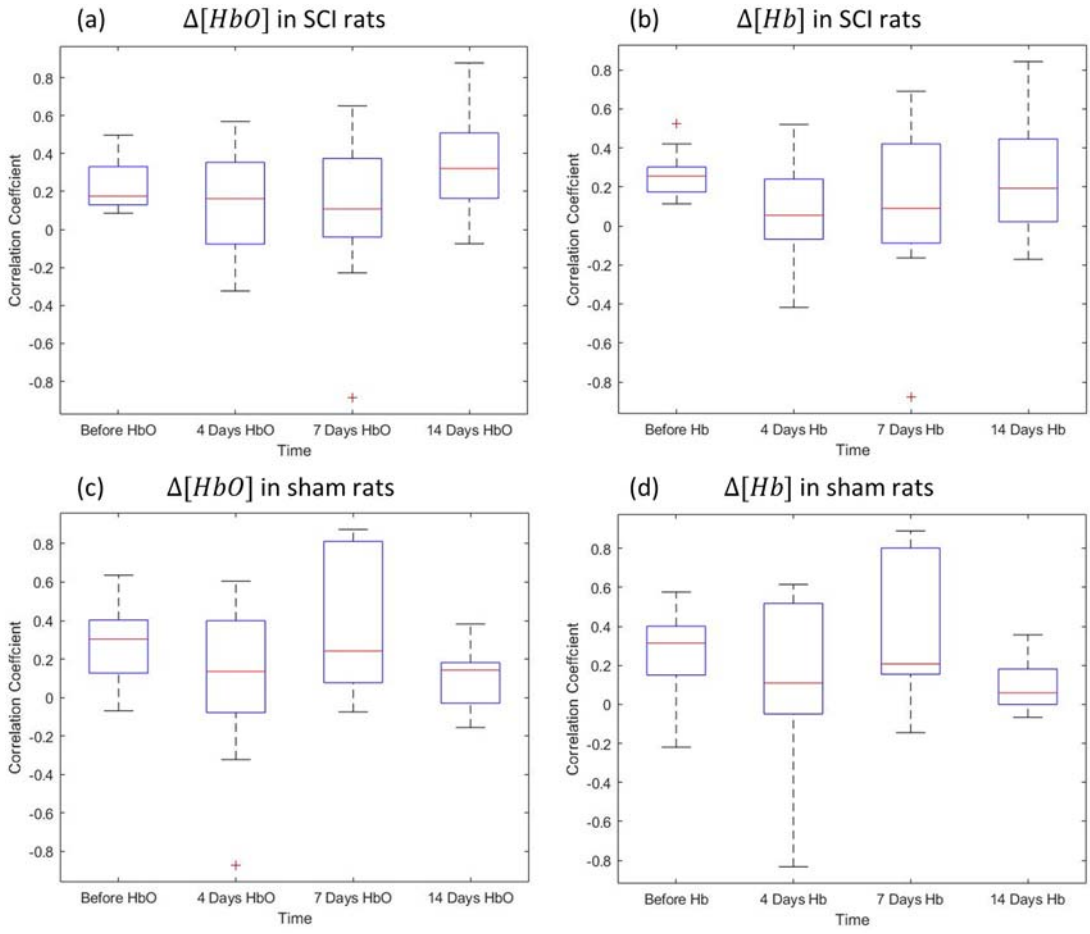

Figure A3 Correlation between front feet channels and rear feet channels over time. (a) Δ[HbO] in SCI rats (b) Δ[Hb] in SCI rats (c) Δ[HbO] in sham rats (d) Δ[Hb] in sham rats.